NPS-67-85-003

NAVAL POSTGRADUATE SCHOOL

Monterey, California

THESIS

MOLECULAR BACK FLOW
FROM THE EXHAUST PLUME
OF A SPACE-BASED LASER

by

Scott E. McCarty

June 1985

Thesis Advisor: A. E. FUHS

Approved for Public Release, Distribution Unlimited

Prepared for: LtCol. Douglas Kline
Code SDIO/DE
Strategic Defense Initiative Organization
Washington, D.C. 20301-7100

NAVAL POSTGRADUATE SCHOOL

Monterey, California

Commodore R.F. Shumaker
Superintendent

David Schrady
Provost

This thesis prepared in conjunction with research supported in part by the Strategic Defense Initiative Organization, Washington, D.C.

Released as a
Technical Report by:

UNCLASSIFIED

SECURITY CLASSIFICATION OF THIS PAGE (When Data Entered)

REPORT DOCUMENTATION PAGE		READ INSTRUCTIONS BEFORE COMPLETING FORM
1. REPORT NUMBER NPS-67-85-003	2. GOVT ACCESSION NO.	3. RECIPIENT'S CATALOG NUMBER
4. TITLE (and Subtitle) Molecular Back Flow from the Exhaust Plume of a Space-based Laser		5. TYPE OF REPORT & PERIOD COVERED Master's Thesis; June 1985 6. PERFORMING ORG. REPORT NUMBER
7. AUTHOR(s) Scott E. McCarty		8. CONTRACT OR GRANT NUMBER(s) DARPA ORDER 4573 See Block 18
9. PERFORMING ORGANIZATION NAME AND ADDRESS Naval Postgraduate School Monterey, California 93943-5100		10. PROGRAM ELEMENT, PROJECT, TASK AREA & WORK UNIT NUMBERS
11. CONTROLLING OFFICE NAME AND ADDRESS Naval Postgraduate School Monterey, California 93943-5100		12. REPORT DATE JUNE 1985 13. NUMBER OF PAGES 54
14. MONITORING AGENCY NAME & ADDRESS(if different from Controlling Office) LtCol. Douglas Kline Code SDIO/DE Strategic Defense Initiative Organization Washington, D.C. 20301-7100		15. SECURITY CLASS. (of this report) UNCLASSIFIED 15a. DECLASSIFICATION/DOWNGRADING SCHEDULE

16. DISTRIBUTION STATEMENT (of this Report)

Approved for Public Release, Distribution Unlimited

17. DISTRIBUTION STATEMENT (of the abstract entered in Block 20, if different from Report)

18. SUPPLEMENTARY NOTES

The research reported herein was initiated under the sponsorship of Defense Advanced Research Projects Agency. During the course of the work the project was transferred to Strategic Defense Initiative Organization.

19. KEY WORDS (Continue on reverse side if necessary and identify by block number)

Spacecraft Contamination, Chemical Lasers, Rarefied Gas Dynamics

20. ABSTRACT (Continue on reverse side if necessary and identify by block number)

Back flow from the exhaust of a chemical laser in low earth orbit may be detrimental to the integrity and operation of the selfsame system. Difficulties arise in the calculation of exhaust plume properties and molecular flux as the gas expands from continuum to free-molecular flow. The solution of the governing Boltzmann equation is exceedingly complex; similarly, numerical solutions such as the Direct Simulation Monte Carlo technique require prohibitive amounts of computer

DD FORM 1 JAN 73 1473 EDITION OF 1 NOV 65 IS OBSOLETE

S/N 0102-LF-014-6601

UNCLASSIFIED

SECURITY CLASSIFICATION OF THIS PAGE (When Data Entered)

processing time. An alternate method of the assessment of molecular flux is presented in which the continuous transition from viscous to collisionless flow is approximated by a suitably defined breadkown surface. The molecular flux incident on a given area of the spacecraft surface is determined by integration of flux from all significant portions of the breakdown surface. Results are presented for exhaust plumes of various stagnation and exit plane conditions emanating from an axisymmetric ring nozzle.

Approved for public release; distribution is unlimited.

Molecular Back Flow from the Exhaust Plume of a Space-based Laser

by

Scott E. McCarty
Lieutenant Commander, United States Navy
A.B., Stanford University, 1976

Submitted in partial fulfillment of the
requirements for the degree of

MASTER OF SCIENCE IN AERONAUTICAL ENGINEERING

from the

NAVAL POSTGRADUATE SCHOOL
June 1985

ABSTRACT

Back flow from the exhaust of a chemical laser in low earth orbit may be detrimental to the integrity and operation of the selfsame system. Difficulties arise in the calculation of exhaust plume properties and molecular flux as the gas expands from continuum to free-molecular flow. The solution of the governing Boltzmann equation is exceedingly complex; similarly, numerical solutions such as the Direct Simulation Monte Carlo technique require prohibitive amounts of computer processing time. An alternate method of the assessment of molecular flux is presented in which the continuous transition from viscous to collisionless flow is approximated by a suitably defined breakdown surface. The molecular flux incident on a given area of the spacecraft surface is determined by integration of flux from all significant portions of the breakdown surface. Results are presented for exhaust plumes of various stagnation and exit plane conditions emanating from an axisymmetric ring nozzle.

TABLE OF CONTENTS

LIST OF FIGURES

ACKNOWLEDGEMENTS

I would like to thank my thesis advisor, Dr. Allen E. Fuhs, for his insightful guidance and assistance from inception to completion of this work. Additionally, I appreciate the timely suggestions and comments of Dr. Joseph Falcovitz during the latter stages of this project. Most of all, I wish to say thank you to my wife JillAnne, whose unflagging confidence and love are ever my source of inspiration. My love to you, Jill.

1. INTRODUCTION

Advancing satellite and spacecraft technology will soon enable the deployment of an array of space-based laser systems. Among the lasers being considered are chemical lasers of the hydrogen halide class. Before their deployment may be realized, however, important questions remain to be answered. Major concerns are the possible contamination and system degradation of low earth orbit spacecraft by laser exhaust back flow. One design of a spacecraft laser is that of a long cylinder, its power output device located at one end, as in Figure 1.1.

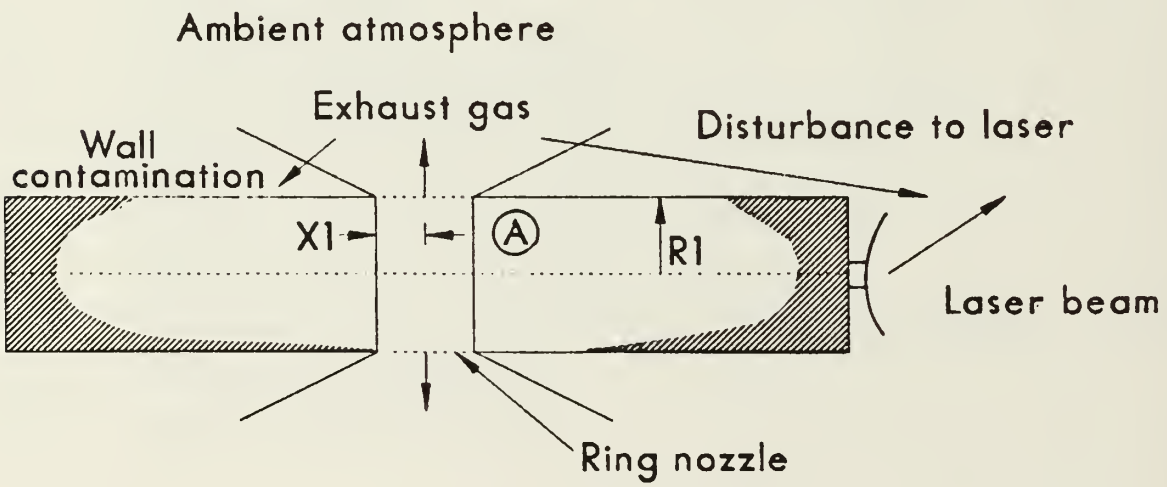

Figure 1.1 Spacecraft Laser.

The exhaust gas is released through a ring nozzle and undergoes rapid three-dimensional axisymmetrical expansion. However, a number of molecules in the expanding plume may have thermal velocity components directed back toward the spacecraft of sufficient magnitude to overcome the mean flow velocity. As certain molecular species in the exhaust plume of a chemical laser may be corrosive to the spacecraft surface, the molecular backscatter from the jet must be determined to assess potential hazards to the spacecraft.

Considerable difficulty arises in the analysis of the flow field of the exhaust jet as it expands rapidly from continuum flow conditions at the nozzle exit plane into the near-vacuum conditions of low earth orbit. In the region where an exhaust plume transitions from continuum to free-molecular flow, a microscopic approach must be taken in the flow analysis. Properly, temporal changes in molecular distribution functions in physical and velocity space must be related to molecular collision parameters. In such analysis the only applicable equation is the Boltzmann equation [Ref. 1], viz.,

$$\frac{\partial(nf)}{\partial t}+u_i \frac{\partial(nf)}{\partial x_i}+F_i \frac{\partial(nf)}{\partial u_i} = \int_{-\infty}^{\infty} \int_{0}^{4\pi} n^2(ff_1'-ff_1)g\sigma \, d\Omega du_1 \quad (1.1)$$

Here, n is the number density, $f(u_i, x_i, t)$ is the normalized distribution function, u_i is molecular velocity, σ is a differential collision cross section, $d\Omega$ is an element of solid angle, F_i is an external force per unit mass, and du is an element of velocity space. The subscript 1 denotes the molecular collision partner and the prime denotes a post-collision value. The left-hand side of the Boltzmann equation represents the change in the number of particles in a phase space element from convection of molecules across the surface of this space due to molecular velocity u_i and external forces F_i. The right-hand side of the equation represents the change in the number of molecules in a phase space element due to particle-to-particle collisions. The Boltzmann equation has been the subject of extensive investigation; however, the complexity of the problem has thus far yielded analytical solutions only to simplified models of a specific nature [Refs. 2,3,4].

For instance, the Chapman-Enskog method of solution of the Boltzmann equation assumes the distribution function f is perturbed by a small amount from the Maxwellian form. The distribution function is then expressed as a power series in ε, a parameter regarded as a measure of mean collision time [Ref. 5].

Approximations to the Boltzmann equation by Hilbert, Burnett, and others consists of expanding f in powers of λ/a, where λ is the mean free path at a point in the flow field and a is a typical macroscopic

dimension of the flow geometry. In the first approximation to the Boltzmann equation, the left-hand side of equation 1.1 is omitted, and the result is a nonlinear integral equation. Higher approximations satisfy inhomogeneous integral equations [Ref. 6]. However, the validity of the above methods is confined to flow of small Knudsen numbers, i.e., $a >> \lambda$.

A numerical approach to the solution of the Boltzmann equation proposed by Bird [Ref. 7] is the Direct Simulation Monte Carlo (DSMC) method, which entails the computer modeling of a real gas flow by several thousand simulated molecules. Continuum flow solutions (e.g., the method-of-characteristics) are used to compute flow field properties to the point at which continuum flow theory is no longer valid. Beyond, flow is simulated on a microscopic scale, molecule-by-molecule. Velocity components and spatial coordinates of each of thousands of molecules are modified over small increments of time until a steady-state solution is determined. A shortcoming of the Direct Simulation Monte Carlo technique is that such a solution may be obtainable only after a great number of iterations of molecular collision algorithms, requiring prodigious amounts of computer processing time.

In order to significantly reduce the computational time required for molecular back flow analysis, while obtaining results of the correct order of magnitude, an alternate approach to the problem is presented herein.

II. METHODOLOGY

Consider the gas jet of Figure 2.1, exiting an axisymmetric ring nozzle into a near-vacuum. The gas undergoes Prandtl-Meyer expansion in which the flow is turned, Mach number increases, and density decreases until ambient pressure is reached.

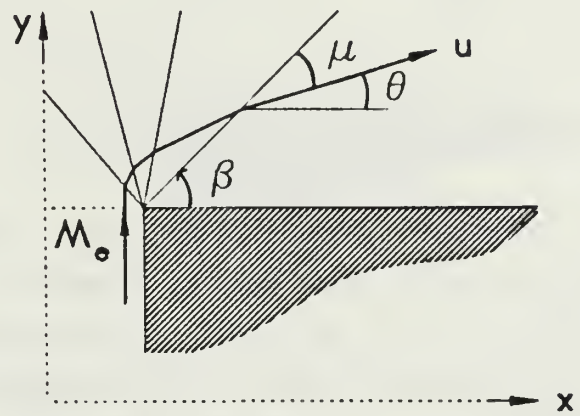

Figure 2.1 Prandtl-Meyer Expansion.
Region A of Figure 1 is expanded in this Figure.

At some point along any streamline in such a flow, there is a breakdown of continuum flow theory [Ref. 8]. Although the transition from viscous to free-molecular (collisionless) flow is actually continuous, a boundary where the transition begins may be approximated in three dimensions by a breakdown surface. We wish to evaluate the magnitude of molecular efflux from the breakdown surface toward the surface of the spacecraft. In reality, molecules crossing the breakdown surface in the direction of the spacecraft enter a transition region in which molecular collisions are highly likely to occur, as depicted in Figure 2.2.

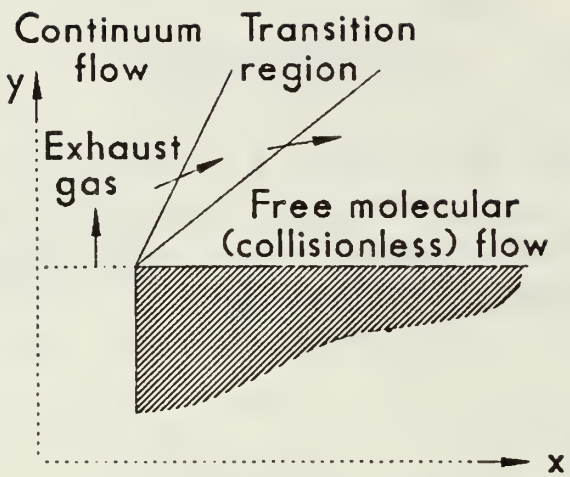

Figure 2.2 Exhaust Flow Breakdown.

However, within the transition region, translational equilibrium of the expanding flow ceases to exist, and thermal properties of the gas, in effect, remain as they were at the onset of breakdown. Therefore, although molecular collisions occur between the breakdown surface and the free-molecular boundary, it is assumed that effusion of molecules toward the spacecraft from the breakdown surface is equivalent to that of the transition region. Hence, this analysis is concerned with determination of flux incident on the spacecraft from a defined breakdown surface.

Bird [Ref. 9] has defined a "breakdown parameter" for steady flow as

$$P = \frac{u}{\rho\nu}\left|\frac{d\rho}{ds}\right| \qquad (2.1)$$

where ν is collision frequency per molecule, ρ is density, u is flow speed, and s is distance along a streamline. The breakdown parameter is thus a modified Knudsen number relating mean free path to density scale length. The onset of breakdown occurs when the value of P is approximately 0.05. We define r as the distance from the fan vertex in

the Prandtl-Meyer expansion and show that P may be expressed explicitly as a function of r and Mach number. The locus of the breakdown surface may thus be determined. The nozzle lip, at which point the Prandtl-Meyer expansion waves are centered, is a singularity point which is also the origin of lines of constant-P, as shown in Figure 2.3.

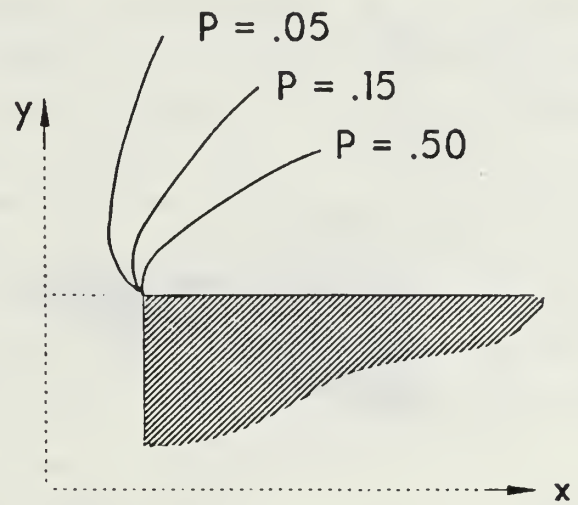

Figure 2.3 Contours of Constant-P.

As the nozzle lip is approached, uncertainties in flow field analysis increase. Here, we are concerned only with flow properties of the gas located more than a few tens of mean free paths from the nozzle lip singularity. As the gas flow proceeds through the Prandtl-Meyer expansion, the value of r on the breakdown surface increases as the local Mach number increases. Properties of the flow at any point along the breakdown surface may be determined as a function of stream flow speed. Further, the molecular flux from a given element of area on the breakdown surface is a function only of local Mach number and the angle between the flux vector and mean flow direction. Thus, from any element on the breakdown surface, the molecular flux incident on an element of area on the spacecraft surface may be determined.

At some point along the breakdown surface, the Mach number is sufficiently high that the backward flux effusion toward the spacecraft

surface is virtually nil, and consideration of flux from points further out on the breakdown surface is unnecessary. This point is shown in Figure 2.4 at the intersection of the breakdown surface defined by P = 0.05 and the expansion wave corresponding to this limiting Mach number.

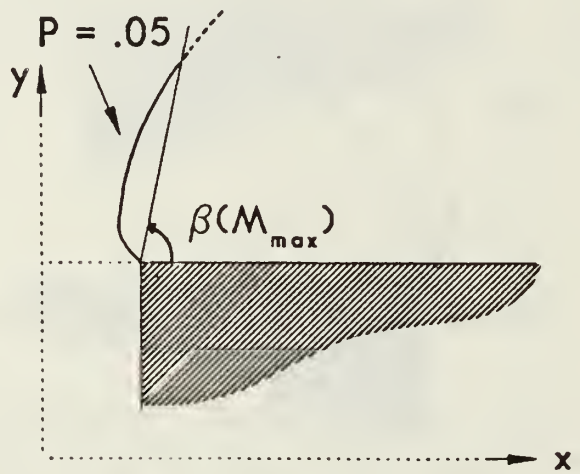

Figure 2.4 Extent of Significant Portion of Breakdown Surface as Defined by the Limiting Mach Number.

The total incident flux at any point on the spacecraft surface is calculated by integration over all those portions of the breakdown surface from which significant flux is received.

III. SOLUTION

A. EXHAUST GAS PROPERTIES

In the schematic representation of a low earth orbit spacecraft laser system of Figure 1.1, pertinent dimensions shown are the spacecraft radius R1 and half-width of the exhaust nozzle X1. The exhaust jet of a hydrogen fluoride laser consists primarily of four molecular species: hydrogen fluoride, hydrogen, deuterium fluoride, and helium. Laser cavity molar flow rates and gas properties [Refs. 10,11,12,13] assumed for the calculations which follow are weighted averages representative of typical laser cavity parameters rather than those of a specific operating point. These parameters are as follows:

molecular weight, $\mathcal{M}$	7.4 kg/kmole
molecular diameter, δ	2.52×10^{-10} m
specific heat ratio, γ	1.493
stagnation density, ρ_t	0.01 to 0.1 kg/m^3
stagnation temperature, T_t	2200 K
exit Mach number, M_e	3.0 to 5.0

B. PRANDTL-MEYER EXPANSION

Laser exhaust gas exits the spacecraft from a centrally-located axisymmetric ring nozzle and undergoes two-dimensional isentropic expansion. The following relations are assumed valid at any point in the isentropic flow field [Ref. 14]:

$$p = \rho RT \tag{3.1}$$

$$R = \mathcal{R}/\mathcal{M} \tag{3.2}$$

$$T_t = T[1+(\gamma-1)M^2/2] \tag{3.3}$$

$$\rho_t = \rho[1+(\gamma-1)M^2/2]^{1/(\gamma-1)} \tag{3.4}$$

$$a = \sqrt{\gamma RT} \tag{3.5}$$

Local temperature, density, and Mach number are denoted by T, ρ, and M. The stagnation temperature T_t and specific heat ratio γ are each constant in the flow field. R is the gas constant per unit mass, $\mathcal{R}$ is the universal gas constant, and a is local sonic speed.

Figure 2.1 depicts a streamline of exhaust flow, with Mach number M_θ at the nozzle exit plane, undergoing Prandtl-Meyer expansion as it leaves the nozzle. The angle between the streamline and a given Mach wave is a function of the local Mach number, related by

$$\sin \mu = 1/M \tag{3.6}$$

Also,

$$\beta = \theta + \mu \tag{3.7}$$

In equation 3.7, θ is the angle between the spacecraft surface and the flow streamline; β is the angle between the spacecraft surface and the tail of the Prandtl-Meyer expansion fan. Owczarek [Ref. 15] gives the total angle that the flow is turned from its direction at the exit plane as

$$\theta_1-\theta_2 = -(\nu_1-\nu_2) \tag{3.8}$$

where the angle of turn is equal to $\theta_1 - \theta_2$. Values for ν are given by the Prandtl-Meyer function

$$\nu(M) = \sqrt{(\gamma+1)/(\gamma-1)}\ \tan^{-1}\sqrt{(\gamma-1)(M^2-1)/(\gamma+1)} - \tan^{-1}\sqrt{M^2-1} \tag{3.9}$$

In Figure 2.1, $\theta_1 = 90°$ and $M_1 = M_\theta$.

C. THERMALLY SCATTERED FLUX

It is assumed that the molecules in any small element of volume in the expanding flow possess a Maxwellian velocity distribution. Noeller [Ref. 16] shows that the fraction of molecules in such a volume element that fly into the space angle $d\omega$, as depicted in Figure 3.1, is

$$(dn_\tau/n_\tau)_{d\omega,dc} = \pi^{-3/2} c^2 e^{-(c^2+u^2-2cu\cos\psi)}\, d\omega dc \qquad (3.10)$$

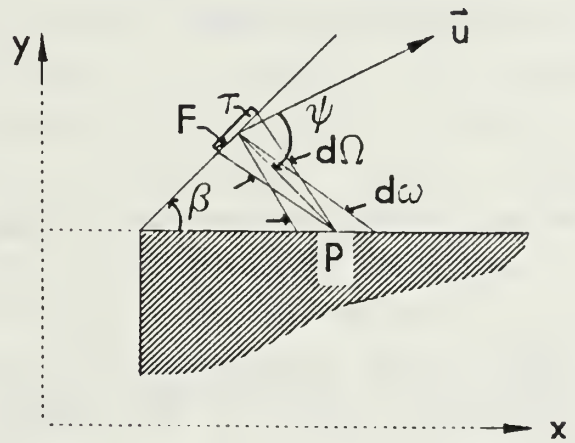

Figure 3.1 Flux Geometry.

Here, u is the stream velocity, c is the inertial flow velocity (i.e., thermal velocity plus stream velocity), and ψ is the angle between the direction of flight and the mean flow direction. Flow speeds in this analysis have been non-dimensionalized with respect to the most probable molecular thermal speed, c_m, where

$$c_m = \sqrt{2RT} \qquad (3.11)$$

Thus,

$$u = Ma/\sqrt{2RT} = M\sqrt{\gamma RT}/\sqrt{2RT} = \sqrt{\gamma/2}M \qquad (3.12)$$

The number density of molecules reaching a point P from the volume τ is

$$dn_P = (dn_\tau/d\omega)d\Omega \tag{3.13}$$

where $d\Omega$ is the solid angle of the surface F from P. Analogously, we may define the incident molecular flux in the vicinity of P arriving from the surface F as

$$dj_P = (dj_F/d\omega)d\Omega \tag{3.14}$$

where

$$(dj_F/d\omega) = n_\tau c_m \pi^{-3/2} c^3 e^{-(c^2+u^2-2cu\cos\psi)} dc \tag{3.15}$$

Hence,

$$(dj_P/d\Omega) = \int_0^\infty n_\tau c_m \pi^{-3/2} c^3 e^{-(c^2+u^2-2cu\cos\psi)} dc \tag{3.16}$$

The evaluation of this integral is given in Appendix A. Thus,

$$dj_P = n_\tau c_m \pi^{-3/2} e^{-u^2}\left[(1+u^2\cos^2\psi)/2+(\sqrt{\pi}/2)(u\cos\psi)\right.$$
$$\left.(e^{u^2\cos^2\psi})\,\mathrm{erfc}(-u\cos\psi)(u^2\cos^2\psi + 3/2)\right] d\Omega \tag{3.17}$$

The local number density is given by

$$n = \rho(N/\mathcal{M}) \tag{3.18}$$

where N is Avogadro's number. From equations 3.4 and 3.18,

$$n_\tau = \frac{\rho_t(N/\mathcal{M})}{\left[1+(\gamma-1)M^2/2\right]^{1/(\gamma-1)}} \tag{3.19}$$

From equations 3.3 and 3.11,

$$c_m = \sqrt{2RT_t/\left[1+(\gamma-1)M^2/2\right]} \tag{3.20}$$

The total flux arriving at point P from the breakdown surface is found by integrating equation 3.17 over the entire solid angle $d\Omega$ within which the surface F appears from P.

From equations 3.12 and 3.17-3.20, the flux emanating from a small surface element is a function only of local Mach number and the angle off the mean flow direction, ψ. The flux is a maximum in the direction of $\vec{u}$, decreasing rapidly as ψ increases. From equation 3.17, values of $(dj_P/d\Omega)$ were calculated for various Mach numbers as a function of ψ. Results are shown in Figure 3.2. Values along the ordinate are $\text{flux}_{\psi,M}/\text{flux}_{\psi=0,M=3}$, i.e., the ratio of flux directed at an angle ψ from the mean flow direction to the magnitude of flux at $\psi = 0°$, M = 3.0. For example, for local flow at Mach 3.0, flux at a back flow angle of 180 degrees is approximately seven orders of magnitude less than flux in the stream flow direction. Similarly, at Mach 14.5, flux directly opposing the stream flow is nearly eighty orders of magnitude below the maximum value.

D. DETERMINATION OF BREAKDOWN SURFACE

A parameter for the determination of continuum flow breakdown is given in equation 2.1. Falcovitz [Ref. 17, Appendix B] evaluates the breakdown parameter P along streamlines of a centered rarefaction fan. A non-dimensional gradient is defined as

$$\kappa(M) = \frac{r}{\rho}\left|\frac{d\rho}{ds}\right| \tag{3.21}$$

whose value for a Prandtl-Meyer fan is

$$\kappa(M) = 2\sqrt{M^2-1}/M(\gamma+1) \tag{3.22}$$

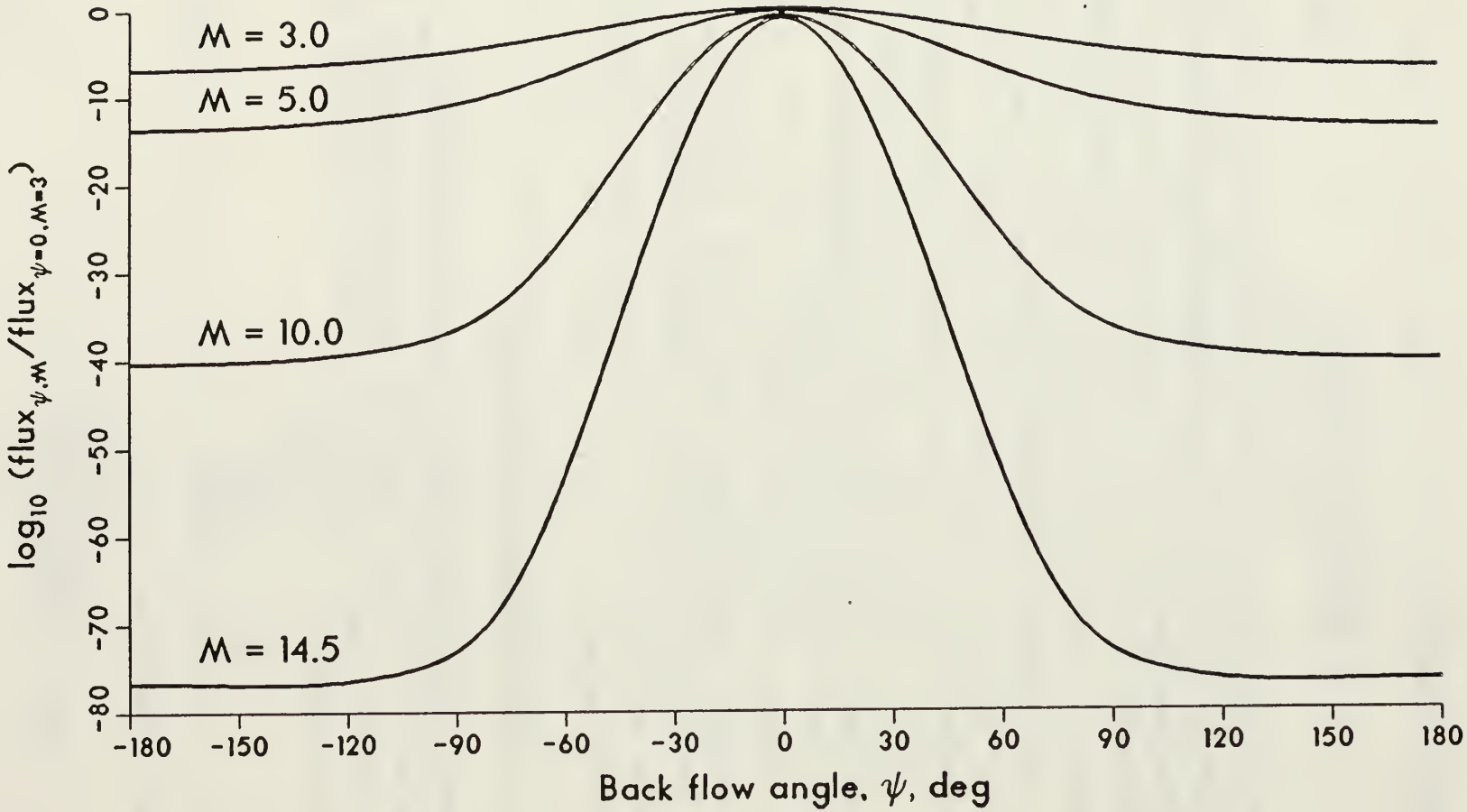

Figure 3.2 Flux Ratio versus Back Flow Angle, ψ, as a Function of Mean Flow Mach Number, M.

Bird [Ref. 18] gives the following relations for the average thermal speed $\bar{c}$, mean free path λ, and collision frequency ν:

$$\bar{c} = 2c_m/\sqrt{\pi} \tag{3.23}$$

$$\lambda = (\sqrt{2}\pi\delta^2 n)^{-1} \tag{3.24}$$

$$\nu = \bar{c}/\lambda \tag{3.25}$$

Substitution of equations 3.5, 3.11, and 3.22-3.25 into equation 2.1 yields

$$P = \frac{\sqrt{(\gamma/\pi)(M^2-1)}}{2(\gamma+1)r\delta^2 n} \tag{3.26}$$

Substitution of equation 3.18 into equation 3.26 gives

$$P = \frac{\sqrt{(\gamma/\pi)(M^2-1)}\left[1+(\gamma-1)M^2/2\right]^{1/(\gamma-1)}}{2(\gamma+1)r\delta^2 \rho_t (N/\mathcal{M})} \tag{3.27}$$

To determine the location of the breakdown surface, P is set equal to 0.05 in equation 3.27. We may now solve explicitly for the distance r of the breakdown surface from the vertex of the expansion fan. As a function of local Mach number,

$$r = \frac{10\sqrt{(\gamma/\pi)(M^2-1)}\left[1+(\gamma-1)M^2/2\right]^{1/(\gamma-1)}}{(\gamma+1)\delta^2 \rho_t (N/\mathcal{M})} \tag{3.28}$$

From evaluation of the Prandtl-Meyer function for the flow fields under consideration, it is found that the maximum Mach numbers reached in the expansion to the ambient pressure of low earth orbit are well in excess of one hundred. However, the molecular back flow from areas along the breakdown surface with flow speeds of this magnitude is negligible. Thus, for efficiency of computation, it is necessary to estimate the maximum Mach number M_{max} which will bear significantly in the

present analysis. An estimate of $M_{max} = 15.0$ was arrived at in the following manner. For the gas under consideration, the Prandtl-Meyer function (equation 3.9) was evaluated for M = 15.0. For flow exiting the nozzle at $M_e = 3.0$, the angle through which the flow is turned (equation 3.8) is approximately 50°. Therefore, the back flow angle for molecules from this flow to reach a point in the plane parallel to the spacecraft surface is approximately 40° off the mean flow direction. Evaluation of equation 3.16 with the appropriate values gives

$$\log_{10}(\text{flux}_{\psi=40°}/\text{flux}_{\psi=0°})_{M = 15.0} \sim -30.0 \tag{3.29}$$

That is, the flux directed toward a plane parallel to the spacecraft surface from flow at Mach 15.0 is thirty orders of magnitude less than the flux in the mean flow direction. Moreover, the magnitude of flux arriving at the spacecraft surface will be less than this value. Thus M = 15.0 is used as an *a priori* estimate of M_{max}. Subsequent calculations confirm that loss of accuracy is not incurred using this estimate.

E. BACK FLOW GEOMETRY

Molecular back flow geometry is presented in Figure 3.3. Two-dimensional projections onto the x-y plane and y-z plane are shown in Figures 3.4 and 3.5. From Phillips [Ref. 19], the angle ψ between the mean flow stream and a point P on the spacecraft surface is given by

$$\cos\psi = \frac{\vec{L}\cdot\vec{u}}{|L||u|} \tag{3.30}$$

where $\vec{L}$ is the vector from a point B on the breakdown surface to a point P on the spacecraft. The magnitude of u is equal to the product of local Mach number and sonic speed. Define the vector from the origin to P as $\vec{P}$, the vector from the origin to B as $\vec{B}$, and unit vectors in the x, y, and z directions as $\hat{x}$, $\hat{y}$, and $\hat{z}$.

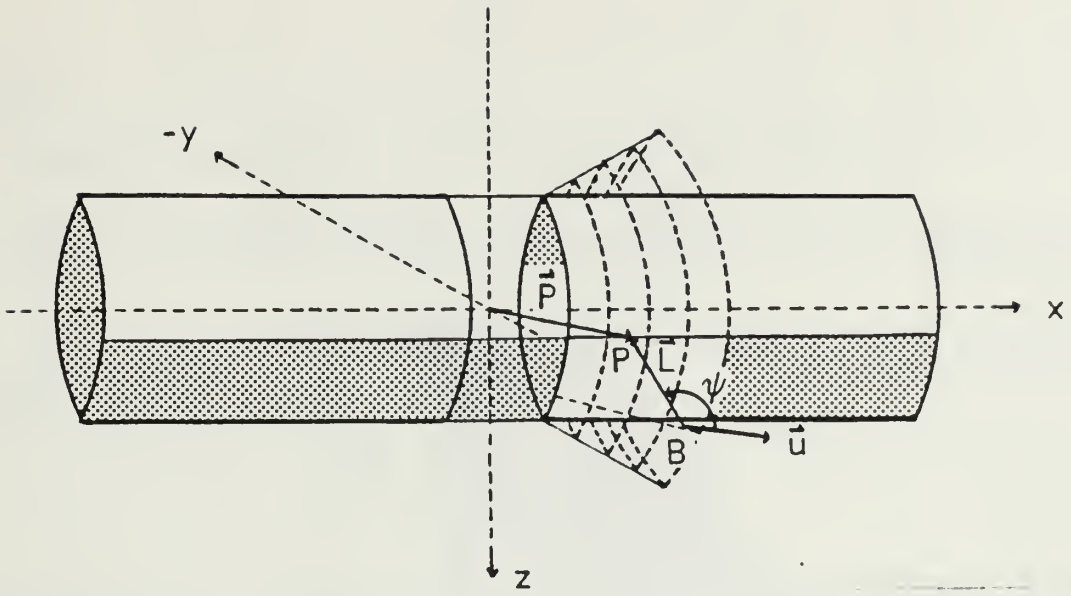

Figure 3.3 Back Flow Geometry.

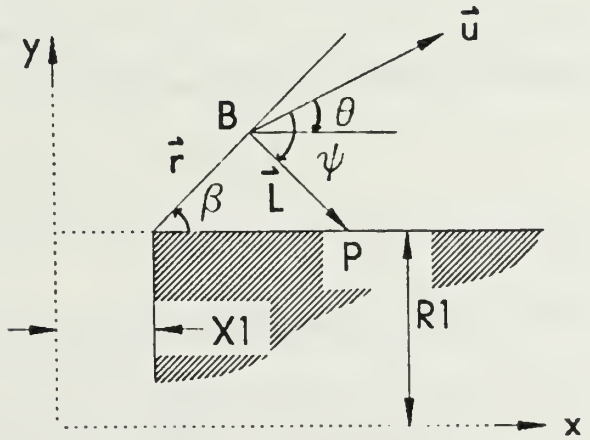

Figure 3.4 Back Flow Geometry: x-y plane.

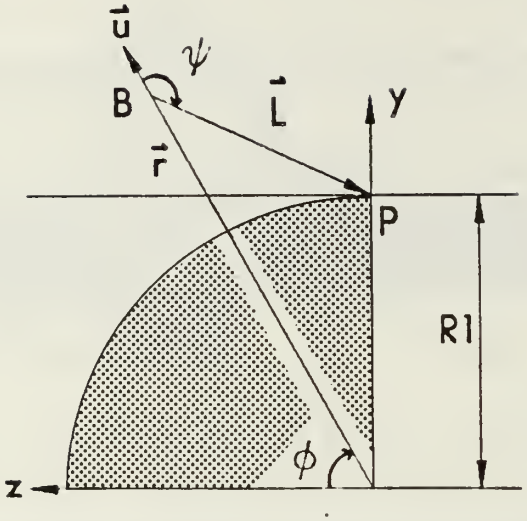

Figure 3.5 Back Flow Geometry: y-z plane.

From Figures 3.3, 3.4, and 3.5, the following relations hold:

$$\vec{P} = x\hat{x} + R1\hat{y} \tag{3.31}$$

$$\vec{B} = (X1 + r\cos\beta)\hat{x} + [(R1 + r\sin\beta)\sin\phi]\hat{y} + [(R1 + r\sin\beta)\cos\phi]\hat{z} \tag{3.32}$$

$$\vec{u} = (u\cos\theta)\hat{x} + (u\sin\theta\sin\phi)\hat{y} + (u\sin\theta\cos\phi)\hat{z} \tag{3.33}$$

$$\vec{L} = \vec{P} - \vec{B} = (x - X1 - r\cos\beta)\hat{x} + [R1 - (R1 + r\sin\beta)\sin\phi]\hat{y} - [(R1 + r\sin\beta)\cos\phi]\hat{z} \tag{3.34}$$

$$|\vec{L}| = \{(x - X1 - r\cos\beta)^2 + [(R1 - (R1 + r\sin\beta)\sin\phi]^2 + [(R1 + r\sin\beta)\cos\phi]^2\}^{1/2} \tag{3.35}$$

Hence,

$$\cos\psi = \{(u\cos\theta)(x - X1 - r\cos\beta) + (u\sin\theta\sin\phi)$$

$$[R1 - (R1 + r\sin\beta)\sin\phi] - (u\sin\theta)(R1 + r\sin\beta)\cos^2\phi\} / |\vec{L}||\vec{u}| \quad (3.36)$$

The solid angle $d\Omega$ within which an element of the breakdown surface appears from the point P is

$$d\Omega = (\vec{L}\cdot\hat{n}d\sigma)/|\vec{L}|^3 \quad (3.37)$$

where $\hat{n}$ is the unit vector normal to the breakdown surface and $d\sigma$ is an element of area on the breakdown surface. Phillips [Ref. 20] gives

$$\hat{n}d\sigma = \frac{\partial\vec{r}}{\partial r} \times \frac{\partial\vec{r}}{\partial\phi}\, drd\phi \quad (3.38)$$

where $\vec{r}$ is the vector along the Mach wave for a specified Mach number to the point B on the breakdown surface (Figure 2.4). The term dr denotes an incremental distance along the breakdown surface. With reference to the coordinate system of Figures 3.3, 3.4, and 3.5:

$$\vec{r} = (r\cos\beta)\hat{x} + (r\sin\beta\sin\phi)\hat{y} + (r\sin\beta\cos\phi)\hat{z} \quad (3.39)$$

$$\frac{\partial\vec{r}}{\partial r} = (\cos\beta)\hat{x} + (\sin\beta\sin\phi)\hat{y} + (\sin\beta\cos\phi)\hat{z} \quad (3.40)$$

$$\frac{\partial\vec{r}}{\partial\phi} = (r\sin\beta\cos\phi)\hat{y} - (r\sin\beta\sin\phi)\hat{z} \quad (3.41)$$

Thus,

$$\hat{n}d\sigma = \left[(-r \sin^2 \beta)\hat{x} + (r \sin \beta \cos \beta \sin \phi)\hat{y} + (r \sin \beta \cos \beta \cos \phi)\hat{z}\right] dr d\phi \qquad (3.42)$$

and

$$\vec{L}\cdot\hat{n}d\sigma = \Big\{(x - X1 - r \cos \beta)(-r \sin^2 \beta) + (r \sin \beta \cos \beta \sin \phi)\left[R1 - (R1 + r \sin \beta)\sin \phi\right] - (r \sin \beta \cos \beta \cos \phi)(R1 + r \sin \beta)\cos \phi\Big\} dr d\phi \qquad (3.43)$$

The solid angle $d\Omega$ (equation 3.37) may now be determined, and the flux from an element of breakdown surface to an element of area near point P (equation 3.17) calculated. The total flux is

$$dj_P = 2\pi^{-3/2} \int_{\phi_{min}}^{\pi/2} \int_{r_{min}}^{r_{max}} n_\tau c_m e^{-u^2} \left[(1+u^2\cos^2\psi)/2 + (\sqrt{\pi}/2)(u \cos \psi)(e^{u^2\cos^2 \psi})\operatorname{erfc}(-u \cos \psi)(u^2\cos^2 \psi + 3/2)\right] d\Omega \qquad (3.44)$$

Note that flow symmetry with respect to the y-axis requires integration only from $\phi = \phi_{min}$ to $\phi = 90°$. Twice this result gives the value for total flux.

F. SPATIAL INTEGRATION OF FLUX

The independent variable used in calculations thus far is local Mach number. For given stagnation parameters and exit plane Mach number, the continuum flow breakdown surface and all pertinent flow properties may be determined as has been shown. The FORTRAN program 'FLUX' (Appendix C) was written to perform the calculations presented herein. In the program, equation 3.44 is evaluated over the extent of the breakdown surface contributing flux to a given target area on the surface of the spacecraft. Only areas of the breakdown surface whose y-components are greater than the spacecraft radius R1

in Figure 3.5 will contribute flux to a line of points along the spacecraft surface defined by y = R1, z = 0. This constraint may be expressed

$$(R1 + r \sin \beta)\sin \phi > R1 \tag{3.45}$$

Having chosen the value of M_{max}, a maximum value for distance from the nozzle lip r_{max} is defined by equation 3.28. This value will in turn define a minimum value of ϕ for the integration procedure, given by

$$\phi_{min} = \sin^{-1}[R1/(R1 + r_{max})] \tag{3.46}$$

Included in Appendix C is a flow chart of the program 'FLUX'. The integration algorithm begins with the input of constants, gas properties, and spacecraft geometry. An exit Mach number, maximum Mach number, and an incremental step value dM are chosen, and a string of target points P are selected on the surface of the spacecraft along the line y = R1, z = 0.

Calculations begin for a target point near the nozzle lip. In order to avoid the singularity at the nozzle lip, the value of M is initialized as (M_e+dM) in a plane near $\phi = \phi_{min}$. The ϕ-plane in which integration begins is defined by values assigned to ϕ_{min} and $d\phi$. In this constant-ϕ plane, Mach number is incremented by dM and the constraint of relation 3.45 is checked. When a value of r is reached such that relation 3.45 is satisfied, the location of the point B, pertinent flow parameters, the back flow angle ψ, and the incremental flux from B toward the target point are calculated. The value of M is incremented and the process is iterated.

A flux magnitude of one molecule per square meter per second arriving in the vicinity of a given target point is used as the minimum value for which calculations proceed in a constant-ϕ plane.

That is, if

$$(dj_P)_{M,\phi} < 1 \text{ per } m^2 \text{ per sec} \qquad (3.47)$$

then the value of ϕ is incremented by $d\phi$, M is reset to M , and iteration begins in a new plane of constant-ϕ. This process continues through $\phi = 90°$. Total incident flux near a given target point is equal to twice the sum of the incremental flux values thus calculated. A new target point is selected and the entire procedure is repeated.

IV. RESULTS

Calculations were performed as described above for exit Mach numbers of 3.0, 4.0, and 5.0, and exhaust plume stagnation densities of 0.01 and 0.1 kg/m^3. A constant stagnation temperature of 2200 K was used in all calculations. Table 1 indicates some of the limiting values calculated for the stated initial conditions. Maximum and minimum distances of the breakdown surface from the nozzle lip are given by r_{max} and r_{min}. M_{max} is that Mach number along the breakdown surface at which the flux to any target area on the surface becomes less than one molecule per square meter per second. Note that the maximum Mach number for which this constraint is reached is M = 12.8. Therefore, the *a priori* estimate of M = 15.0 did not limit the accuracy of back flow calculations. The two right-hand columns give the mean free path λ at the nozzle exit plane and the ratio of r_{min} to λ. The latter parameter gives a relative indication of the "closest point of approach" of the breakdown surface to the singularity at the nozzle lip.

TABLE 1

Exit Plane and Breakdown Surface Parameters.

M_e	ρ_t, kg/m^3	r_{max}, cm	r_{min}, cm	M_{max}	λ, cm	r_{min}/λ
3.0	.01	81.53	.1730	11.65	.0047	37.1
3.0	.10	13.00	.0173	12.80	.0005	37.1
4.0	.01	27.63	.5592	9.35	.0111	50.2
4.0	.10	3.57	.0559	9.85	.0011	50.2
5.0	.01	18.38	1.4878	8.60	.0236	63.0
5.0	.10	2.29	.1488	9.00	.0024	63.0

The most salient data presented in Table 1 are the values for r , which in essence define the extent of the breakdown surface contributing flux to the surface of the spacecraft. Values for r are generally less than one meter. Moreover, for the cases of higher stagnation

densities and exit Mach numbers, the total significant efflux from the breakdown surface toward the spacecraft originates from within only a few centimeters from the nozzle lip.

Figures 4.1, 4.2, and 4.3 show the magnitude of flux incident on the spacecraft surface for exit Mach numbers of 3.0, 4.0, and 5.0, respectively. In each figure, values along the abscissa (distance from the nozzle lip) range from one millimeter to ten meters. For each set of initial conditions considered, flux in the plane of the nozzle exit reaches a maximum near the nozzle lip, generally well within ten centimeters. The variance of flux within this distance of the lip is not more than about one order of magnitude. Beyond, incident flux to the spacecraft decreases rapidly; at a point ten meters from the nozzle exit the back flow is generally three to four decades less than the maximum values.

The magnitude of molecular back flow is a strong function of exit plane Mach number, exhibiting inverse proportionality. The variance of back flow with stagnation density is less pronounced. Near the nozzle lip, the spacecraft receives a slightly greater molecular flux from the higher-stagnation density exhaust plume. However, at distances greater than one meter from the nozzle lip, flux received by the spacecraft is virtually independent of stagnation density, and becomes a function only of exit Mach number.

Figure 4.4 depicts the sensitivity of flux magnitude to assumed values of the breakdown parameter P. As P is modified, the general locus of the breakdown surface changes as shown in Figure 2.3. Maximum flux magnitude appears to be insensitive to increasing values of P. However, changes in the shape of the flux distribution curve do occur. As the assumed value of P increases, flux near the nozzle lip is increased and the point of maximum flux moves inward toward the nozzle lip. Beyond the point of maximum flux, though, the decrease in back flow to the surface of the spacecraft decays more rapidly for higher values of P.

Calculations were also performed to assess the validity of approximating the breakdown surface by the expansion wave corresponding to M_{max}, as shown in Figure 2.4. From results shown in Figure 4.5, it appears that little loss of accuracy is incurred in making this assumption.

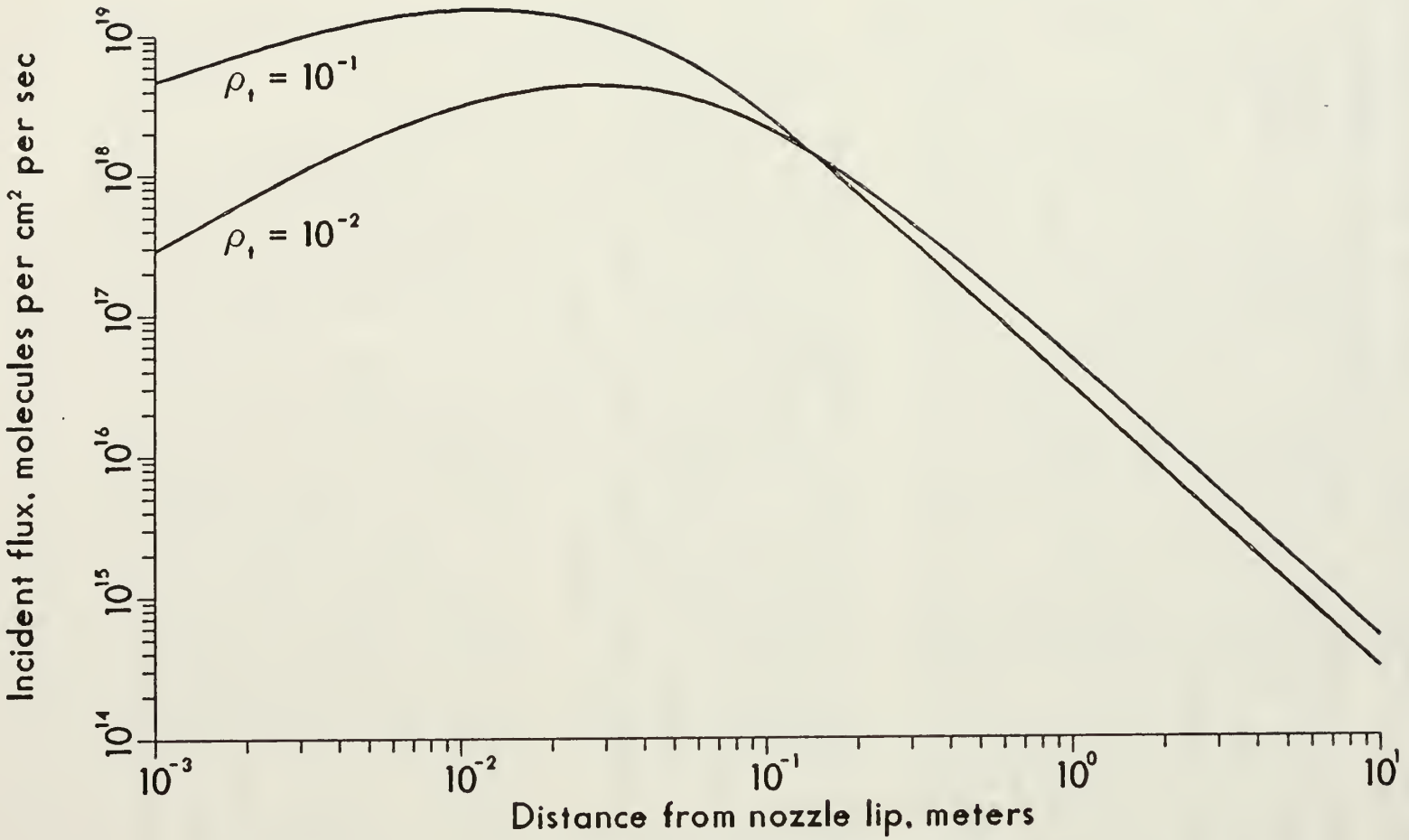

Figure 4.1 Molecular Flux in Plane of Nozzle Exit;
Stagnation Temperature = 2200 K, Exit Mach Number = 3.0.
Plume Stagnation Densities are given in kg/m³.

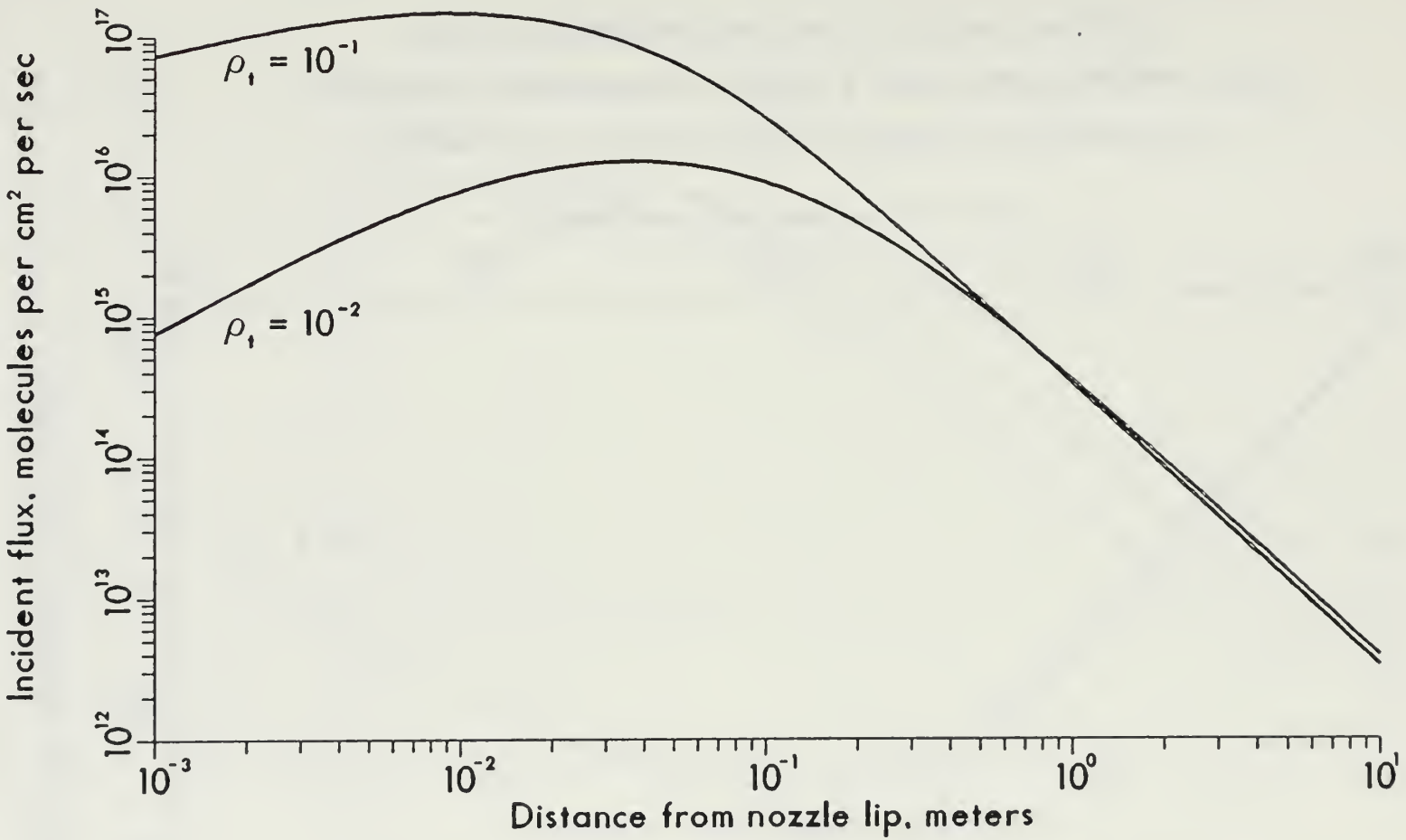

Figure 4.2 Molecular Flux in Plane of Nozzle Exit;
Stagnation Temperature = 2200 K, Exit Mach Number = 4.0.
Plume Stagnation Densities are given in kg/m³.

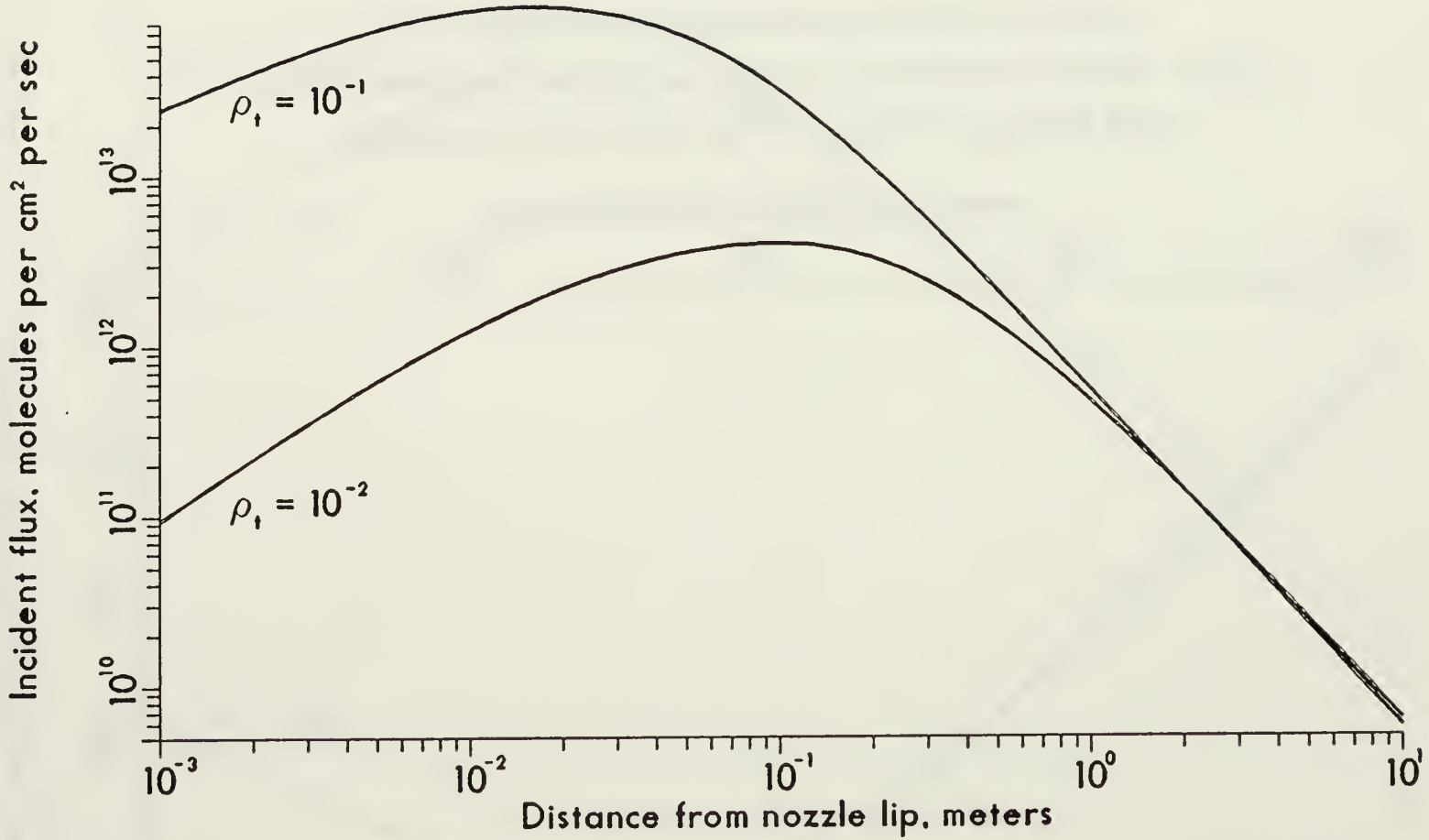

Figure 4.3 Molecular Flux in Plane of Nozzle Exit:
Stagnation Temperature = 2200 K, Exit Mach Number = 5.0.
Plume Stagnation Densities are given in kg/m³.

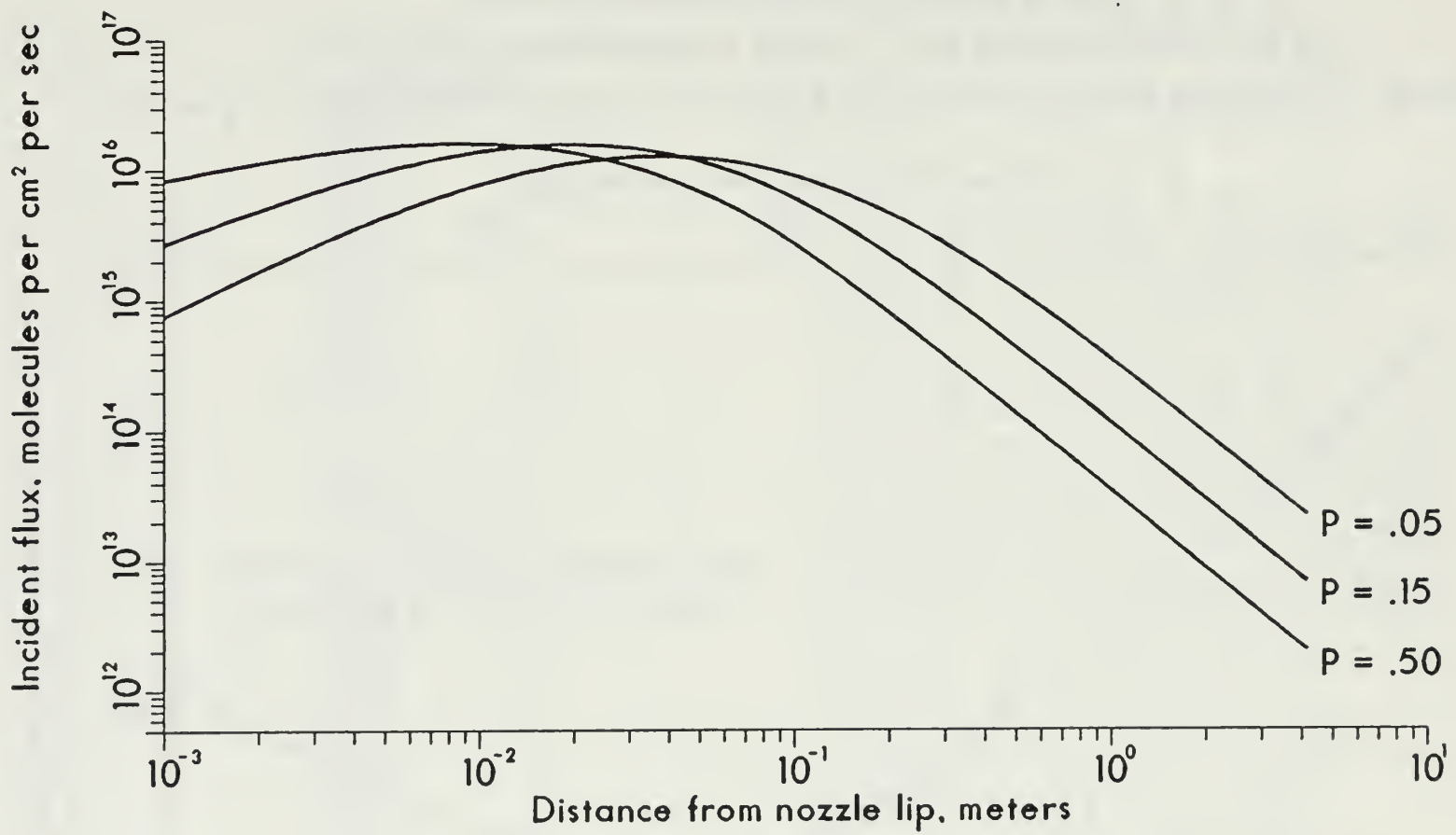

Figure 4.4 Sensitivity of Flux to Assumed Value of Breakdown Parameter, P; Stagnation Temperature = 2200 K, Exit Mach Number = 4.0. Plume Stagnation Density = 10^{-2} kg/m³.

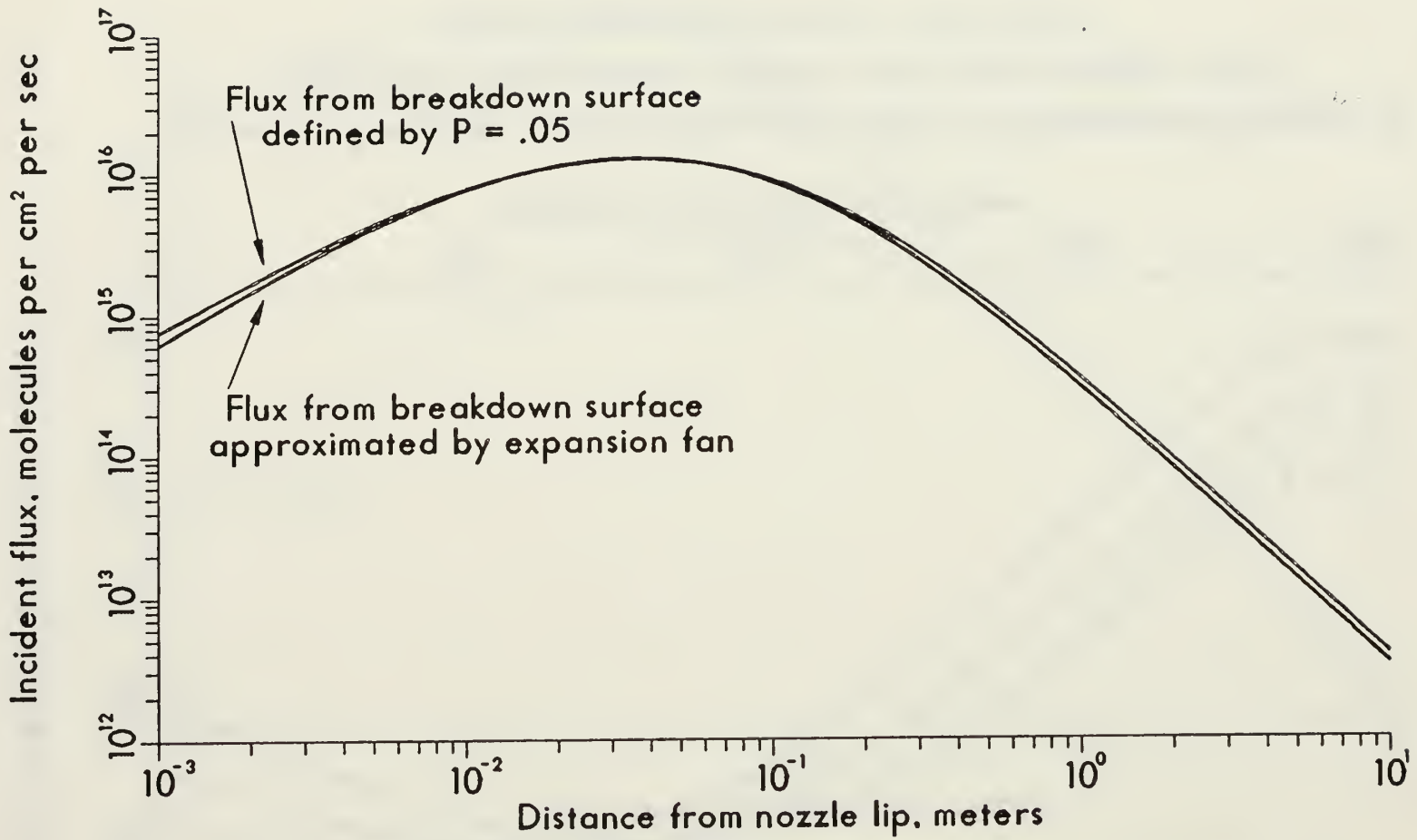

Figure 4.5 Comparison of Flux from Actual and Approximated Breakdown Surfaces; Stagnation Temperature = 2200 K, Exit Mach Number = 4.0. Plume Stagnation Density = 10^{-2} kg/m³.

V. CONCLUSIONS

The data presented in Figures 4.1, 4.2, and 4.3, and Table 1 indicate that for both effusion and reception of molecular flux, the region in the immediate vicinity of the nozzle lip is of critical importance. Therefore, efforts to minimize the molecular back flow to the spacecraft surface warrant attention to this region. In theory, rather straightforward and uninvolved modifications to the spacecraft structure near the exhaust nozzle would significantly decrease incident back flow. Comparison of Figures 4.1, 4.2, and 4.3 shows that minimization of back flow is contingent upon raising the exit Mach number of the exhaust jet to a value as high as feasible. With all other parameters constant, increasing the exit Mach number from 3.0 to 5.0 decreases flux to any given area on the spacecraft surface by approximately five orders of magnitude.

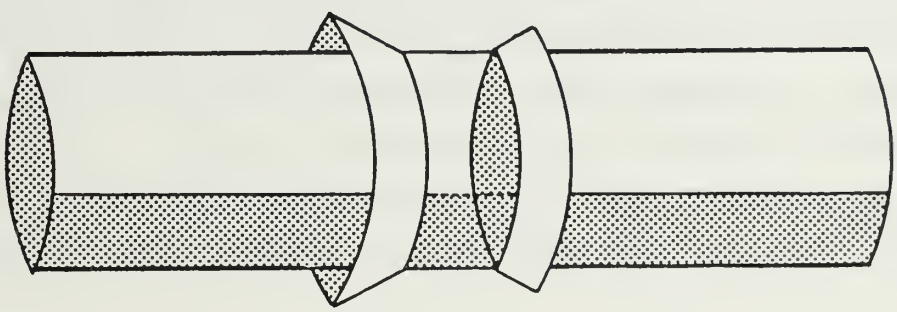

Figure 5.1 Exhaust Nozzle Modification.

Shown in Figure 5.1 is the addition of a rim located at either edge of the nozzle, encircling the spacecraft. Benefits of such an

arrangement would be twofold. Most importantly, the effective nozzle expansion ratio is increased, thereby increasing exit Mach number. Additionally, the back flow angle for molecular flux to reach a given area on the spacecraft is greater than that for the design in which the nozzle exit plane is flush with the spacecraft surface.

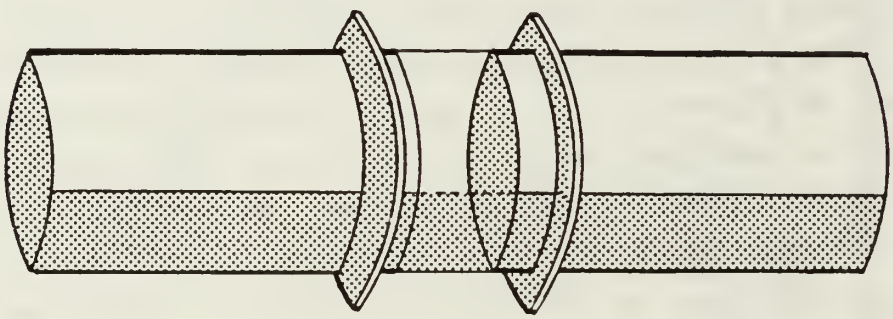

Figure 5.2 Exhaust Nozzle Modification.

Small vertical barriers encircling the spacecraft near the nozzle lip as shown in Figure 5.2 would also be effective in significantly reducing incident flux. Added without regard to increasing area ratio or exit Mach number, the "fences" would act simply to block a high percentage of the molecular effusion from the breakdown surface. In light of the values of r_{max} given in Table 1, it is conceivable that such a modification, even if only a few centimeters in height, could be extremely effective.

VI. RECOMMENDATIONS

One of the limitations of the foregoing analysis is that physical and thermodynamic properties of the exhaust plume are taken to be weighted averages of the properties of the constituent molecular species. Realistically, the number density, mean free path, and collision rates of each molecular species will not necessarily be equal to one another at any specified point in the flow field.

Further, in this analysis, the effect on the exhaust plume of the atmosphere through which the spacecraft is traveling has been neglected. Although the molecular number densities associated with low earth orbit altitudes are small, the velocity of these molecules relative to a spacecraft advancing in orbit is significant. The relative approach of these atmospheric molecules toward the spacecraft is parallel to the plane of the nozzle exit and therefore nearly perpendicular to the locus of points describing the breakdown surface of the exhaust plume. Collisions between free stream molecules and exhaust gas molecules occurring in the transition region of the exhaust plume will result in a transfer of energy to molecules in this region.

The resolution of each of the limitations above will further improve the accuracy of the results presented in this analysis.

APPENDIX A
ON THE GRADIENT IN CENTERED RAREFACTION FAN

Joseph Falcovitz

Feb. 19, 1985

Purpose: Evaluate the Bird/Knudsen number

$$P = \frac{u}{\rho\nu}\left|\frac{d\rho}{ds}\right|$$

along streamlines of centered rarefaction fan.

Reference: J.A. Owczarek, "Fundamentals of Gas Dynamics"

(1) Mach wave: $\sin\mu = 1/M$

(2) $\beta = \mu + \theta$; θ = streamline angle

For a centered fan, flow field is function of β.

Denote: r = distance from fan vertex

s = coordinate along streamline

ρ = density

ρ_t = stagnation density

Then $(d\rho/ds)$ is a $(-\sin\mu)$ component of $\frac{1}{r}\frac{d\rho}{d\beta}$:

$$(3)\quad \frac{d\rho}{ds} = \frac{1}{r}\frac{d\rho}{d\beta}\sin\mu = -\frac{1}{rM}\frac{d\rho}{d\beta}$$

Denote the non-dimensional gradient:

$$(4)\quad \kappa(M) = \frac{r}{\rho}\frac{d\rho}{ds}$$

Then for a centered fan:

$$(5)\quad \kappa(M) = -\frac{1}{M\rho}\frac{d\rho}{d\beta} = -\frac{1}{M\rho}\frac{d\rho}{dM}\left[\frac{d\beta}{dM}\right]^{-1} = -\frac{1}{M\rho}\frac{d\rho}{dM}\left[\frac{d\mu}{dM}+\frac{d\theta}{dM}\right]^{-1}$$

$$\frac{d\mu}{dM} = -\frac{1}{M^2\cos\mu} = -\frac{1}{M^2(1-1/M^2)^{1/2}} = -\frac{1}{M(M^2-1)^{1/2}}$$

$$\frac{d\theta}{dM} = -\frac{(M^2-1)^{1/2}}{M[1+(\gamma-1)M^2/2]}$$

$$\frac{d\beta}{dM}=\frac{d\mu}{dM}+\frac{d\theta}{dM}= -\frac{(\gamma+1)M}{2(M^2-1)^{1/2}[1+(\gamma-1)M^2/2]}$$

$$\rho_t = \rho[1+(\gamma-1)M^2/2]^{1/(\gamma-1)}$$

$$\frac{d\rho}{dM} = -\rho M[1+(\gamma-1)M^2/2]^{-1}$$

$$\frac{1}{\rho}\frac{d\rho}{dM} = -M[1+(\gamma-1)M^2/2]^{-1}$$

$$(6)\quad \kappa(M) = 2\sqrt{M^2-1}/M(\gamma+1)$$

APPENDIX B
EVALUATION OF INTEGRALS

Given

$$(dj_p/d\Omega) = \int_0^\infty n_\tau c_m \pi^{-3/2} c^3 e^{-(c^2+u^2-2cu\cos\psi)} dc$$

Via the method of Noeller [Ref. 16], the substitution $k = c - u\cos\psi$ is made. The right-hand side of the equation becomes

$$n_\tau c_m \pi^{-3/2} \int_{-u\cos\psi}^\infty (k+u\cos\psi)^3 e^{-k^2} e^{-u^2(1-\cos^2\psi)}\, dk$$

which in expanded form equals

$$n_\tau c_m \pi^{-3/2} e^{-u^2} e^{u^2\cos^2\psi} \left\{ \int_{-u\cos\psi}^\infty k^3 e^{-k^2}\, dk + 3u\cos\psi \int_{-u\cos\psi}^\infty k^2 e^{-k^2}\, dk \right.$$

$$\left. + 3u^2\cos^2\psi \int_{-u\cos\psi}^\infty k e^{-k^2}\, dk + u^3\cos^3\psi \int_{-u\cos\psi}^\infty e^{-k^2}\, dk \right\}$$

The evaluation of these four integrals is as follows:

1. $$\int_{-u\cos\psi}^\infty k^3 e^{-k^2}\, dk = (u^2\cos^2\psi\, e^{-u^2\cos^2\psi} + e^{-u^2\cos^2\psi})/2$$

2. $$\int_{-u\cos\psi}^\infty k^2 e^{-k^2}\, dk = -(u\cos\psi\, e^{-u^2\cos^2\psi})/2 + (\sqrt{\pi}/4)\operatorname{erfc}(-u\cos\psi)$$

3. $$\int_{-u\cos\psi}^\infty k e^{-k^2}\, dk = (e^{-u^2\cos^2\psi})/2$$

4. $$\int_{-u\cos\psi}^{\infty} e^{-k^2}\,dk = (\sqrt{\pi}/2)\mathrm{erfc}(-u\cos\psi)$$

where erfc is the complementary error function. Substitution yields

$$dj_P = n_T c_m \pi^{-3/2} e^{-u^2}\left[(1+u^2\cos^2\psi)/2+(\sqrt{\pi}/2)(u\cos\psi)\right.$$

$$\left.(e^{u^2\cos^2\psi})\mathrm{erfc}(-u\cos\psi)(u^2\cos^2\psi + 3/2)\right] d\Omega$$

APPENDIX C

FORTRAN PROGRAM 'FLUX'

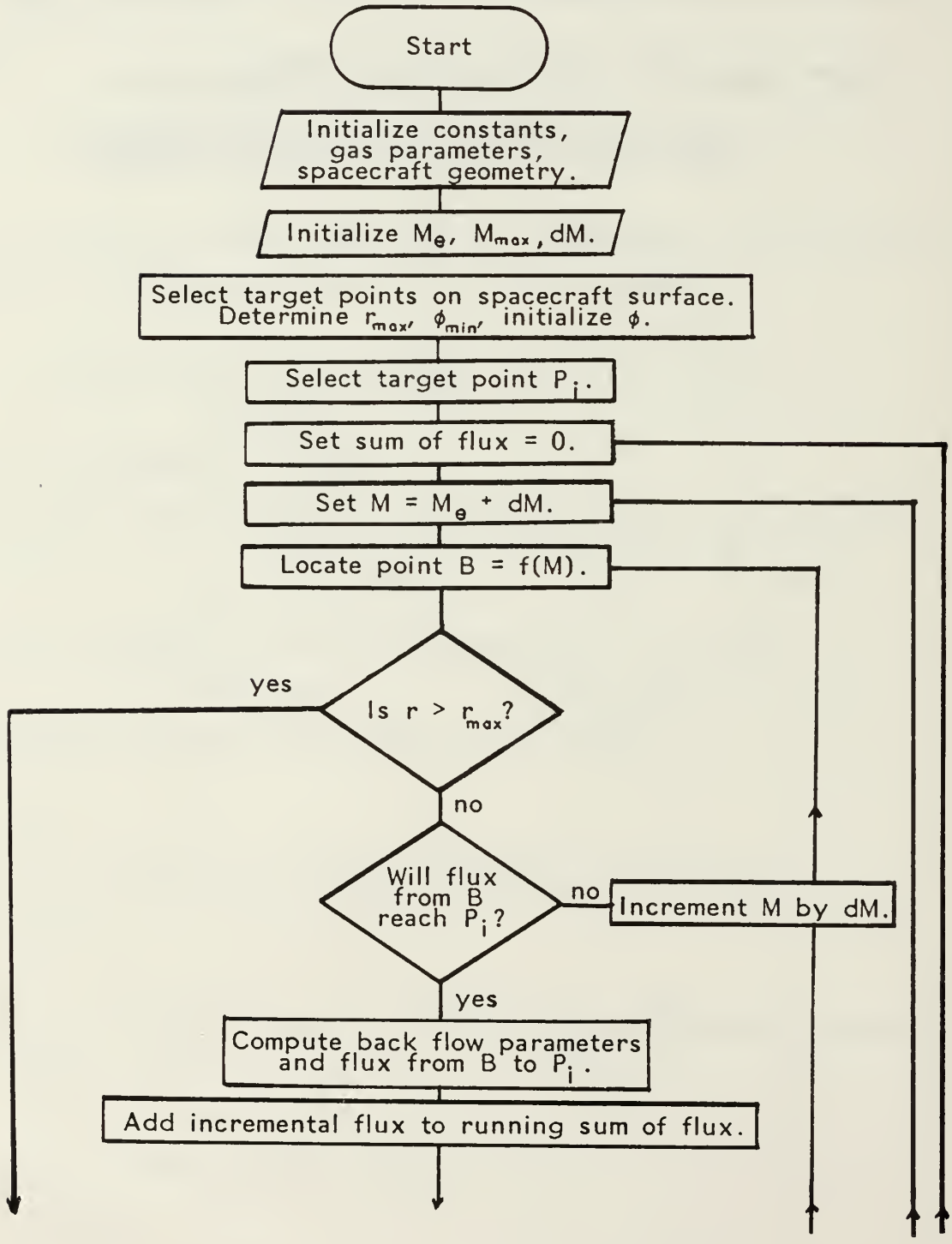

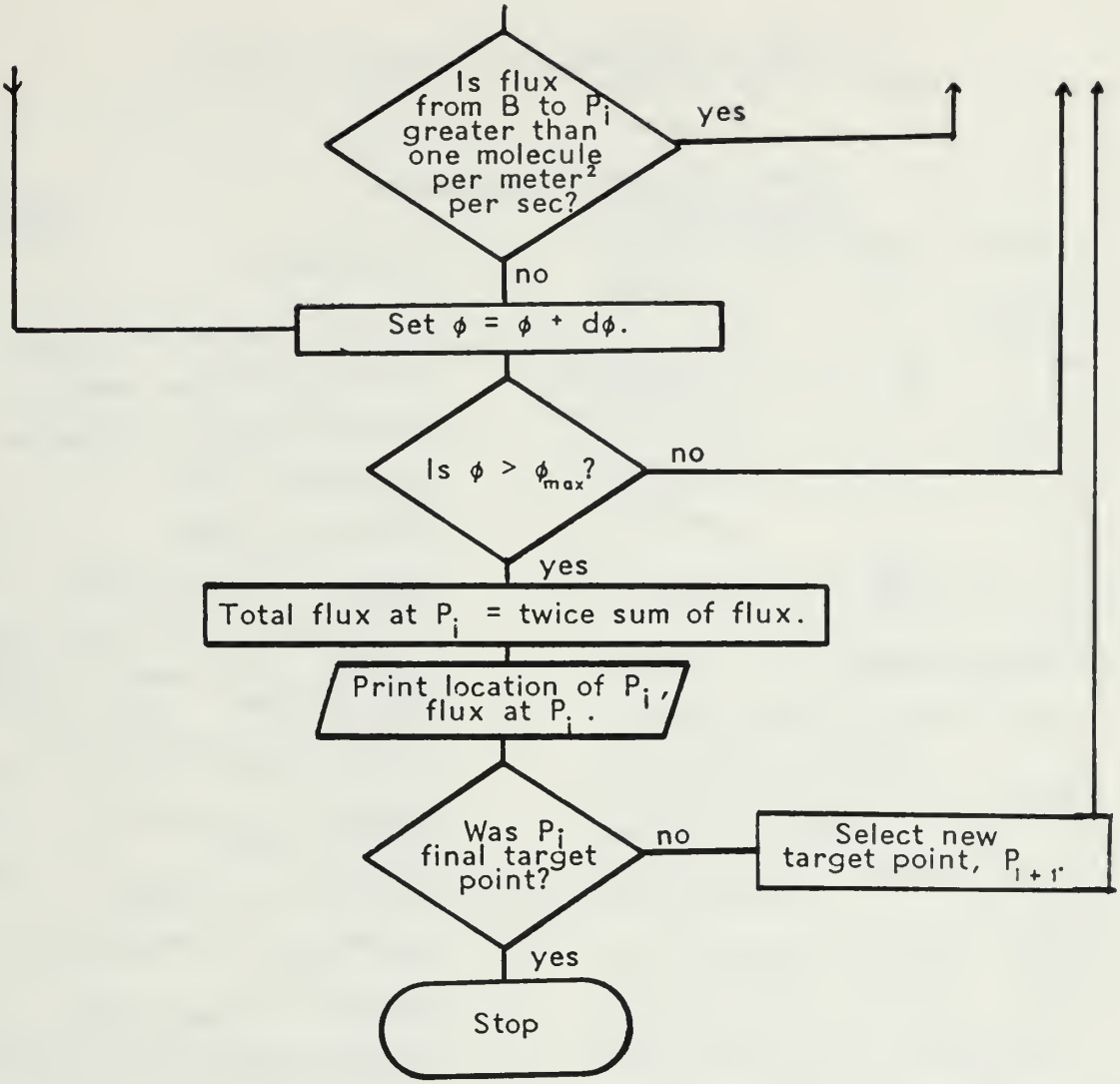
Is flux from B to P_i greater than one molecule per meter^2 per sec?
yes
no
Set $\phi = \phi + d\phi$.
Is $\phi > \phi_{max}$?
no
yes
Total flux at P_i = twice sum of flux.
Print location of P_i, flux at P_i.
Was P_i final target point?
no
Select new target point, P_{i+1}.
yes
Stop

LIST OF SYMBOLS IN PROGRAM "FLUX"

Input Parameters

Symbol	*Name*	*Units*	*Description*
GAMMA	γ		average specific heat ratio
MW	$\mathcal{M}$	kg/kmole	average molecular weight
DELTA	δ	m	average molecular diameter
R1		m	spacecraft radius
X1		m	nozzle half-width
ME	M_e		exit plane Mach number
DM	dM		incremental Mach number step
MMAX	M_{max}		estimate of maximum flow field Mach number
TSTG	T_t	K	stagnation temperature of exhaust plume
DSTG	ρ_t	kg/m^3	stagnation density of exhaust plume
P	P		breakdown parameter
IPHI, PHIDIV			number of ϕ-divisions for integration
IPTS			number of target points
XMIN		m	x-coordinate of target point nearest nozzle lip
XMAX		m	x-coordinate of target point furthest from nozzle lip

Other Parameters

Symbol	*Name*	*Units*	*Description*
PI	π		3.1415926
E	e		2.7182818
RU	universal gas constant	J/mole·K	8314.41
N0	Avogadro's number	molecules per kmole	6.022045×10^{26}

SIGMA	σ	m^2	collision cross section
RG	R	J/kg·K	$R = \mathcal{R}/\mathcal{M}$
XDIV, LRATIO, XCOORD, MM			variables used in determination of intermediate target points
C1			$2/(\gamma - 1)$
C2			$(\gamma + 1)/(\gamma - 1)$
C3			$(\gamma - 1)/(\gamma + 1)$
C4			$(\gamma - 1)/2$
C5			$(\gamma/\pi)^{1/2}$
C6			$1/(\gamma - 1)$
NU1	ν_1	radians	Prandtl-Meyer function at nozzle exit
RMAX	r_{max}	m	value of r corresponding to M_{max}
PHIMIN	ϕ_{min}	radians	minimum value of ϕ used in integration procedure
DPHI	$d\phi$	radians	incremental ϕ-step
PHI	ϕ	radians	spatial coordinate
FLUX	j_P	molecules per m^2 per sec	flux arriving in vicinity of target point
ML	M		local flow Mach number
NU	ν	radians	Prandtl-Meyer function
THETA	θ	radians	angle between spacecraft surface and flow streamline
BETA	β	radians	angle between spacecraft surface and Prandtl-Meyer wave
R	r	m	distance from nozzle lip
DR	dr	m	incremental distance step
MPS	c_m	m/sec	most probable thermal molecular speed, $(2RT)^{1/2}$
UMAG	$\lvert\vec{u}\rvert$		magnitude of stream flow velocity
LDOTU	$\vec{L}\cdot\vec{u}$		variables defined by equations 3.33, 3.34, 3.35, and 3.43.
LMAG	$\lvert L\rvert$		
LNDS	$L\cdot\hat{n}d\sigma$		
PSI	ψ	radians	flux back flow angle
DOMEGA	$d\Omega$	steradians	solid angle subtended by portion of breakdown surface

U	u		dimensionless flow speed, $(\gamma/2)^{1/2}M$
C7			$u \cos \psi$
C8			$u^2 \cos^2 \psi$
C9			e^{-u^2}
C10			$e^{u^2 \cos^2 \psi}$
ND	n_T	molecules/m^3	number density
DFLUX	dj_p	molecules per m^2 per sec	incremental flux directed toward target point
TFLUX	j_p	molecules per cm^2 per sec	total flux incident near target point
MLIM	M_{max}		maximum stream Mach number for which breakdown is significant

```
C PROGRAM FLUX.
C THIS PROGRAM CALCULATES THE MOLECULAR FLUX INCIDENT ON A SURFACE
C FROM EXHAUST FLOW EXITING AN AXISYMMETRIC RING NOZZLE.
      IMPLICIT REAL*8(A-H,L-Z,$)
      DIMENSION ML(500),THETA(500),R(500),U(500),XCOORD(99),LRATIO(99)
      DIMENSION DR(500),NU(500),MPS(500),ND(500),MLMAX(99)
C INITIALIZE CONSTANTS
      ARG = 1.
      PI = 4.*DATAN(ARG)
      E = 2.7182818
      RU = 8314.41
      NO = 6.022045D26
C EXHAUST GAS PROPERTIES
      GAMMA = 1.493
      MW = 7.4
      DELTA = 2.52D-10
      SIGMA = DELTA*DELTA
      RG = RU/MW
C SPACECRAFT GEOMETRY
      R1 = 2.5
      X1 = .5
C FLOW FIELD AND INTEGRATION PARAMETERS
      ME = 4.
      DM = .05
      MMAX = 15.
      TSTG = 2200.
      DSTG = .1
      P = .05
      IPHI = 30
      IPTS = 35
      XMIN = .501
      XMAX = 10.5
      XDIV = DFLOAT(IPTS)
      LRATIO(IPTS) = 0.
      XCOORD(1) = XMIN
      DO 111 I1 = 2,IPTS
      MM = DFLOAT(I1)
      LRATIO(IPTS+1-I1) = DLOG10(MM)/DLOG10(XDIV)
  111 CONTINUE
      WRITE(4,400)IPTS
C CONSTANTS USED IN FLOW FIELD CALCULATIONS
      C1 = 2./(GAMMA-1.)
      C2 = (GAMMA+1.)/(GAMMA-1.)
      C3 = 1./C2
      C4 = 1./C1
      C5 = DSQRT(GAMMA/PI)
```

```
      C6 = 1./(GAMMA-1.)
C CALCULATE PRANDTL-MEYER FUNCTION AT EXIT PLANE
      NU1 = DSQRT(C2)*DATAN(DSQRT(C3*(ME*ME-1.)))-DATAN(DSQRT(ME*ME-1.))
      WRITE(6,600)ME,DSTG,TSTG
  600 FORMAT(//' EXIT MACH:',F5.2,3X,'STAG. DENSITY, KG/M3:',F7.3,3X,'ST
     &AG. TEMP:',F8.2)
      WRITE(6,601)
  601 FORMAT('0',3X,'X',4X,'TOTAL FLUX, PARTICLES/CM2*SEC')
C CALCULATE VALUE OF RMAX FOR SPECIFIED VALUE OF MMAX
      RMAX = (C5*DSQRT(MMAX*MMAX-1.)*(1.+C4*MMAX*MMAX)**C6)/(2.*(GAMMA+1
     &.)*P*SIGMA*DSTG*(NO/MW))
      PHIMIN = DARSIN(R1/(R1+RMAX))
      PHIDIV = DFLOAT(IPHI)
      DPHI = (PI/2.-PHIMIN)/PHIDIV
C SELECT TARGET POINTS ALONG SURFACE
      DO 222 I2 = 1,IPTS
      XCOORD(I2) = XMAX-LRATIO(I2)*(XMAX-XMIN)
      PHI = PHIMIN+DPHI/2.
      FLUX = 0.
  333 I = 0
  444 I = I+1
C SEQUENTIALLY INCREMENT MACH NUMBER BY DM.
C CALCULATE PRANDTL-MEYER FUNCTION.
      ML(I) = ME+DFLOAT(I)*DM
      NU(I) = DSQRT(C2)*DATAN(DSQRT(C3*(ML(I)*ML(I)-1.)))-DATAN(DSQRT(ML
     &(I)*ML(I)-1.))
      THETA(I) = PI/2.-(NU(I)-NU1)
C DETERMINE LOCATION OF POINT ON BREAKDOWN SURFACE; CHECK TO SEE IF IT
C WILL CONTRIBUTE FLUX TO THE TARGET POINT.
      BETA = THETA(I)+DARSIN(1./ML(I))
      R(I) = (C5*DSQRT(ML(I)*ML(I)-1.)*(1.+C4*ML(I)*ML(I))**C6)/(2.*(GAM
     &MA+1.)*P*SIGMA*DSTG*(NO/MW))
      R(I+1) = (C5*DSQRT((ML(I)+DM)**2.-1.)*(1.+C4*((ML(I)+DM)**2.))**C6
     &)/(2.*(GAMMA+1.)*P*SIGMA*DSTG*(NO/MW))
      IF (I.EQ.1) DR(I) = (R(I+1)-R(I))/2.
      IF (I.GT.1) DR(I) = (R(I+1)-R(I-1))/2.
C CALCULATE FLOW PARAMETERS, BACK FLOW ANGLE, SOLID ANGLE AT
C BREAKDOWN POINT
      MPS(I) = DSQRT(2.*RG*TSTG/(1.+C4*ML(I)*ML(I)))
      IF (R(I).GT.RMAX) GO TO 1
      IF ((R1+R(I)*DSIN(BETA))*DSIN(PHI).LT.R1) GO TO 444
      UMAG = MPS(I)*DSQRT(GAMMA/2.)*ML(I)
      LDOTU = UMAG*DCOS(THETA(I))*(XCOORD(I2)-X1-R(I)*DCOS(BETA))+(UMAG*
     &DSIN(THETA(I))*DSIN(PHI))*(R1-(R1+R(I)*DSIN(BETA))*DSIN(PHI))-(UMA
     &G*DSIN(THETA(I))*DCOS(PHI))*(R1+R(I)*DSIN(BETA))*DCOS(PHI)
```

```
      LMAG = DSQRT(DABS((XCOORD(I2)-X1-R(I)*DCOS(BETA)))**2.+DABS((R1-(R
     &1+R(I)*DSIN(BETA))*DSIN(PHI)))**2.+((R1+R(I)*DSIN(BETA))*DCOS(PHI)
     &)**2.)
      PSI = DARCOS(LDOTU/(LMAG*UMAG))
      LNDS = (X1+R(I)*DCOS(BETA)-XCOORD(I2))*R(I)*DSIN(BETA)**2.+(R1-(R1
     &+R(I)*DSIN(BETA))*DSIN(PHI))*R(I)*DSIN(BETA)*DCOS(BETA)*DSIN(PHI)-
     &((R1+R(I)*DSIN(BETA))*DCOS(PHI)*R(I)*DSIN(BETA)*DCOS(BETA)*DCOS(PH
     &I))*DR(I)*DPHI
      DOMEGA = DABS(LNDS/LMAG**3.)
C VARIABLES USED IN CALCULATION OF FLUX FROM BREAKDOWN POINT
      U(I) = ML(I)*DSQRT(GAMMA/2.)
      C7 = U(I)*DCOS(PSI)
      C8 = C7*C7
      C9 = E**(-(U(I)*U(I)))
      C10 = E**C8
      ND(I) = (N0/MW)*DSTG/(1.+C4*ML(I)*ML(I))**C6
C EVALUATE FLUX FROM BREAKDOWN POINT TO TARGET POINT.  CHECK FOR
C SIGNIFICANT FLUX MAGNITUDE.  INCREMENT M UNTIL MMAX REACHED.
      DFLUX = MPS(I)*ND(I)*C9*((1.+C8)/2.+(DSQRT(PI)/2.)*C7*C10*DERFC(-C
     &7))*(C8+1.5))*DOMEGA/PI**1.5
      IF (DFLUX.LT.1.) GO TO 1
      FLUX = FLUX + DFLUX
      IF (I.EQ.1) GO TO 444
      IF (ML(I).GT.ML(I-1)) MLMAX(I2) = ML(I)
      GO TO 444
C INCREMENT PHI BY DPHI; CONTINUE CALCULATIONS IN PLANE OF
C CONSTANT-PHI.  CONTINUE INTEGRATION THROUGH PHI = PI/2.
    1 PHI = PHI+DPHI
      IF (PHI.GT.PI/2.) GO TO 2
      GO TO 333
C EVALUATE TOTAL FLUX.  WRITE RESULTS FOR GIVEN TARGET POINT.
    2 TFLUX = 2.*FLUX/1.D+04
      P0 = XCOORD(I2)-X1
      WRITE(6,602)P0,TFLUX
      WRITE(4,401)P0,TFLUX
  602 FORMAT(' ',F6.3,10X,D10.3)
      IF (I2.EQ.1) GO TO 222
      IF (MLMAX(I2).GT.MLMAX(I2-1)) MLIM = MLMAX(I2)
  222 CONTINUE
      WRITE(6,603)MLIM
  603 FORMAT('0','MAX MACH NUMBER = ',F6.2)
  400 FORMAT('0',I4)
  401 FORMAT(' ',D12.5,1X,D12.5)
      STOP
      END
```

LIST OF REFERENCES

1. Bird, G.A., "Direct Simulation and the Boltzmann Equation", *The Physics of Fluids*, vol. 13, no. 11, 1970, p. 2678.

2. Shidlovskiy, V.P., *Introduction to Dynamics of Rarefied Gases*, Elsevier, 1967, p. 15.

3. Aerospace Research Laboratories Report ARL 73-0134, *A State-of-the-Art Survey of the Mechanics of Rarefied Gas Flows*, by K.S. Nagaraja, September 1973, p. 48.

4. Patterson, G.N., "A Synthetic View of the Mechanics of Rarefied Gases, *AIAA Journal*, vol. 3, no. 4, April 1965, p. 584.

5. Bird, G.A., *Molecular Gas Dynamics*, Clarendon Press, 1976, p.54.

6. Keller, J.B., "On the Solution of the Boltzmann Equation for Rarefied Gases", *Comm. on Appl. Math.*, vol. 1, no. 3, 1948.

7. Op. cit., "Direct Simulation and the Boltzmann Equation", p. 2676.

8. Bird, G.A., *Breakdown of Continuum Flow in Freejets and Rocket Plumes*, paper presented at Twelfth International Symposium on Rarefied Gas Dynamics, Charlottesville, Virginia, 7-11 July 1980.

9. Ibid.

10. Air Force Weapons Laboratories Technical Report AFWL-TR-72-28, *Hydrogen Fluoride Laser Technology Study*, by F. Mastrup, *et al*, October, 1972, p. 91.

11. Williams, R.A., *Handbook of the Atomic Elements*, Philosophical Library, 1970, p. 42.

12. National Aeronautics and Space Administration SP-105, *Vacuum Technology and Space Simulation*, by D.J. Santeler, *et al*, 1966, p. 5.

13. Gordon, A.J., and Ford, R.A., *The Chemist's Companion, A Handbook of Practical Data, Techniques, and References*, Wiley Interscience, 1972.

14. Owczarek, J.A., *Fundamentals of Gas Dynamics*, International Textbook Company, 1964, pp. 153-159.

15. Ibid., pp. 442-443.

16. Noeller, H.G., "Approximate Calculation of Expansion of Gas from Nozzles into High Vacuum", *The Journal of Vacuum Science and Technology*, vol. 3, no. 4, 1966, p. 203.

17. Falcovitz, J., *On the Gradient in Centered Rarefaction Fan*, personal notes, 19 February 1985. (Appendix A)

18. Op. cit., *Molecular Gas Dynamics*, pp. 6, 59, 70.

19. Phillips, H.B., *Vector Analysis*, John Wiley and Sons, Inc. 1933, p. 7.

20. Ibid., p. 94.

INITIAL DISTRIBUTION LIST

		No. Copies
1.	Defense Technical Information Center Cameron Station Alexandria, Virginia 22304-6145	2
2.	Library Code 0142 Naval Postgraduate School Monterey, California 93943-5100	2
3.	Chairman Department of Aeronautics Code 67 Naval Postgraduate School Monterey, California 93943-5100	1
4.	Distinguished Professor Allen E. Fuhs Department of Aeronautics Code 67Fu Naval Postgraduate School Monterey, California 93943-5100	4
5.	LtCol. Douglas Kline Code SDIO/DE Strategic Defense Initiative Organization Washington, D.C. 20301-7100	2
6.	Commanding Officer Attn: Lcdr. Scott E. McCarty Fighter Squadron 101 N.A.S. Oceana Virginia Beach, Virginia 23460	4

21660

Thesis
M16665 McCarty
c.1 Molecular back flow
from the exhaust plume
of a space-based laser.